

Abstract

A numerical model for generating solar radiation maps to be used for the evaluation of different power generation strategies is proposed. The solar radiation model is implemented taking into account the terrain surface with the use of 2-D adaptive meshes of triangles, which are made using a refinement/derefinement procedure in accordance with the variations of terrain surface, orography and albedo. The chosen methodology defines the terrain characteristics with a minimum number of points so that computational cost for a given accuracy is reduced. As we will use the model to find the ideal location to get the maximum power generation, taking into account the effect of shadows for each time step is needed. The solar radiation is first computed for clear-sky conditions, considering the different components of radiation, that is, beam, diffuse and reflected radiations. The real-sky radiation is computed daily starting from the results of clear-sky radiation, in terms of the clear-sky index. The maps of clear-sky index are obtained from a spatial interpolation of observational data that are available for each day at several points of the zone under consideration. Finally, the solar radiation maps of a month are calculated from the daily results. One of the aims of this model is the analysis of the generation possibilities from both, photovoltaic and solar thermal power and the suitability of different locations in Gran Canaria Island (Canary Islands - Spain).

Keywords: solar radiation, clear sky, real-sky, shadows, adaptive meshes, solar power, solar photovoltaics, solar thermal.

1 Introduction

Renewable energies are showing a growing importance as time goes by. The oil shortage and the climate change caused by the global warming have caused a high increase

in the development of the different renewable energies technologies. Between them, solar power has become very important during the last years due to the support of the authorities and to the advances obtained through the research in this field. Part of this research is the development of many numerical models of solar radiation.

There are three groups of factors that determines the interaction of solar radiation with the earth's atmosphere and surface (see e.g. [1, 2]):

1. The Earth's geometry, revolution and rotation (declination, latitude, solar hour angle)
2. Terrain (elevation, albedo, surface inclination and orientation, shadows)
3. Atmospheric attenuation (scattering, absorption) by gases, particles and clouds

Considering the three factors of atmospheric attenuation in the model, it will produce real-sky radiation values. If we omit the cloud attenuation, clear-sky (cloudless) radiation values will be obtained.

Two main groups of spatial models for solar radiation can be found. On one hand there are those models based on the study of data obtained from satellite observations (see e.g., [3]), and, on the other, those based on astrophysical, atmosphere physical and geometrical considerations. Among that latter group, we highlight the works of Šúri and Hofierka [1, 2] regarding a GIS-based solar radiation model.

The main purpose of this paper is the calculation of solar radiation on the terrain [4]. Solar radiation research is important not only in meteorology but also in forestry, agronomy, geography, medicine and, of course, power generation. For solar collectors, the application of our model is straightforward. It can determinate the terrain-induced shading on collectors, although currently it is not oriented to radiation computation on them. We should use the altimetry for shadow modelling and a fixed orientation and inclination of the collectors in order to calculate the solar radiation.

In this work we propose some improvements to the models of Šúri and Hofierka [1, 2] and Montero et al. [4]. The accurate definition of the terrain surface and the produced shadows are studied using an adaptive mesh of triangles. Niewienda et al. [5] propose calculating the GSC (geometrical shading coefficient), the proportion of shaded area of an arbitrarily oriented surface surrounded by shading elements, as a function of time and location. Zakšek et al. [6] propose a solar radiation model based on defining incidence angle by computing normal-to-the-surface tangent plane and direction of the Sun. Since they use a regular grid in their computations, the computational cost of this approach is higher than others using an adaptive discretization.

Other methods [7, 8] do not consider a solid surface and, thus, need a high density of sample points in order to obtain accurate results. In contrast, [4] use a mesh representing a solid surface that actually casts shadows and so it is not as sensitive as the former to the density of sample points. Mesh refinement/derefinement techniques that have been widely used in other scientific problems [9, 10, 11, 12] have been applied. Specifically, this model includes the implementation of the 4-T Rivara's refinement algorithm [13] and derefinement algorithm [14], developed by [10].

In short, our adaptive model allows the refinement of the results of a GIS-based model that would have a high computational cost in accurate local area simulations.

In addition, this model may be connected to a GIS tool as a local solver.

Solar power generation is one of the most important challenges nowadays for engineers. Its contribution to the next future energy scenario is fundamental. The estimation of the actual possibilities of solar power generation in a given place, starts from the accurate knowing of the available radiation. Having this in mind, we have carried out some improvements in the model [4]. To calculate the radiation values for real sky conditions, a typical meteorological year (TMY) for each available measurement stations has been developed following the method used in [15]. The obtained results allow us to estimate the amount of the expected electric power generation, for any day at any place in the island.

2 Terrain surface mesh and detection of shadows

In [4], an adaptive procedure of mesh refinement/derefinement has been carried out using two different derefinement parameters in order to take into account both, orography and albedo. Nested meshes have been used to transfer information along an evolution process (for example, shadow and radiation) from mesh to mesh, when the mesh changes from one step to another (for example, mesh adaption).

To make the mesh generation, the first step consists in the determination of nodes allocated on the terrain surface. Their distribution must be adapted to the orographic and albedo characteristics in order to minimize the number of required nodes for a given accuracy. A sequence of nested meshes $\Gamma = \{\tau_1 < \tau_2 < \dots < \tau_m\}$ is builded from a regular triangulation τ_1 of the rectangular region under study, such that the level τ_j is obtained by a global refinement of the previous level τ_{j-1} with the 4-T Rivara's algorithm [13]. Each triangle of level τ_{j-1} is divided into four subtriangles. The number of levels m of the sequence is determined by the degree of discretization of the terrain, so we can ensure that this regular mesh is able to capture all the orographic and albedo information by an interpolation of the heights and albedo in the nodes of the mesh.

The next step consists of defining a new sequence $\Gamma' = \{\tau_1 < \tau'_2 < \dots < \tau'_{m'}\}$, $m' \leq m$, by applying the derefinement algorithm [10, 14]. By means of two derefinement parameters, ε_h and ε_a , we can determine the accuracy of the approximation to terrain surface and albedo. The absolute difference between the height obtained in any point of the mesh $\tau'_{m'}$ and the corresponding exact height will be lower than ε_h .

The accurate estimation of the solar radiation on a terrain surface needs to take into account the projected shadows. One triangle will be shadowed when, looking at the mesh from the sun, we can find another triangle that totally or partially covers the former. To carry out this analysis, we construct a reference system x', y' and z' , with z' in the direction of the beam radiation (see Figure 1), and the mesh is projected on the plane $x'y'$.

The sun position with respect to a horizontal surface is given by two coordinates, the solar altitude h_0 and the solar azimuth A_0 (see Figure 1), which are calculated as,

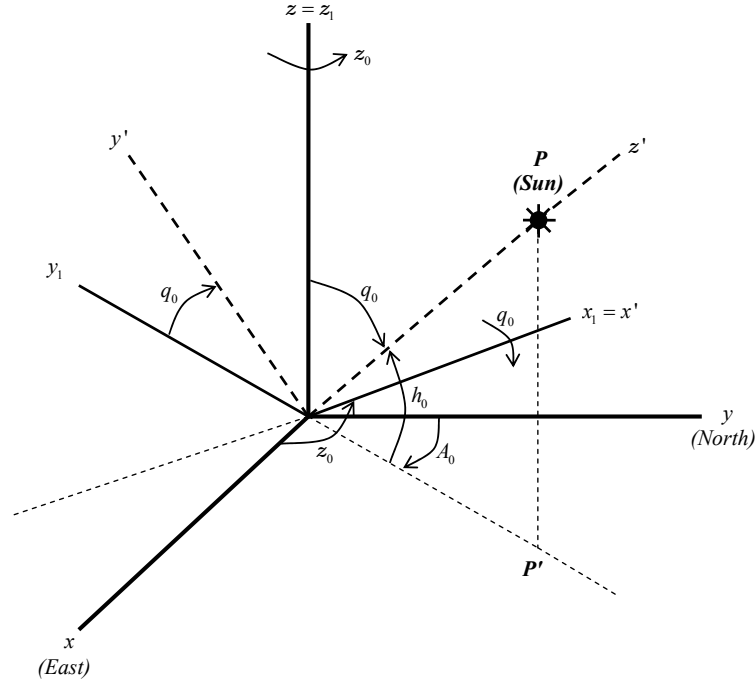


Figure 1: Reference systems and Euler angles

$$\sin h_0 = \cos \varphi \cos \delta \cos T + \sin \varphi \sin \delta \quad (1)$$

$$\cos A'_0 = \frac{\sin \varphi \cos \delta \cos T - \cos \varphi \sin \delta}{\sin h_0} \quad (2)$$

$$\text{if } \sin T > 0, \quad A_0 = -A'_0$$

$$\text{if } \sin T \leq 0, \quad A_0 = A'_0$$

T is the hour angle (rad) obtained from equation (5), φ the latitude in radians and δ the sun declination in radians obtained according to [16],

$$\sin \delta = 0.3978 \sin [j' - 1.4 + 0.0355 \sin(j' - 0.0489)] \quad (3)$$

with j' being the day angle represented in radians as follows,

$$j' = \frac{2\pi j}{365.25} \quad (4)$$

Here j is the day number which varies from 1 on January 1st to 365 on December 31st. The hour angle T (rad) is calculated from the local solar time t expressed in decimal hours on the 24 hour clock as

$$T = \frac{\pi}{12}(t - 12) \quad (5)$$

For each triangle two angles are computed, the azimuth A_N (angle between the horizontal normal projection and East), and γ_N (angle between the normal to the triangle and the horizontal plane). The solar incidence angle δ_{exp} is then computed for each triangle [17, 18].

Thus, we have assumed a constant irradiance on all the points of a given triangle. Once this is done, the intersection between triangles is checked. This analysis involves a high computational cost. To diminish this cost we have considered four warning points for each triangle.

We assign a different level of lighting or shade to each triangle of the mesh depending on the number of warning points that lie inside other triangles. Specifically, a triangle Δ will have an associated lighting factor,

$$L_f = \frac{4 - i}{4} \quad (6)$$

with $i = 0, 1, 2, 3, 4$ being the number of warning points inside other triangles that are in front of Δ . Clearly, L_f is a quantity between 0 and 1. This factor is used below in the estimation of beam and diffuse irradiances.

3 Solar radiation modelling

Starting from the work of Šúri and Hofierka [1, 2], we have proposed both the use of adaptive meshes for surface discretization and a new method for detecting the shadows over each triangle of the surface [4]. Results have been improved by means of the use of TMY extracted from the available measurements stations data [15]. The calculations flow would be:

1. Solar radiation calculation for all the mesh, assuming clear sky conditions
2. TMY calculation for all the involved measurement stations
3. Correction of the solar radiation values using the measured values to reach the real sky conditions

Steps one and three are repeated for each time step and finally the total solar radiation value is obtained integrating all the instantaneous values.

3.1 Solar radiation equations for clear sky

The global solar irradiance comprises three different components: beam, diffuse and reflected irradiances. The first one, partially attenuated by the atmosphere, is not reflected or scattered and reaches the surface directly. The second one is the scattered irradiance that reaches the terrain surface and that goes in all directions and produces no shadows of the inserted opaque objects. The third one is the irradiance which is reflected from the surface onto an inclined receiver and depends on the ground albedo. The relative importance of these three kind of irradiances depends upon the

sky conditions. In sunny days, the diffuse radiation would be no more than the 15% of the global radiation, while on overcast days its importance will be much greater. The reflected or albedo irradiance is the one with the lowest contribution to the global.

3.1.1 Beam radiation

Taking into account [19], we will take the solar constant I_0 as $1367 \text{ (W/m}^2\text{)}$ outside the atmosphere at the mean solar distance. Due to the earth's orbit eccentricity, a correction factor ϵ is applied for calculation of the extraterrestrial irradiance G_0 .

$$G_0 = I_0 \epsilon \quad (7)$$

where $\epsilon = 1 + 0.03344 \cos(j' - 0.048869)$, with j' being the day angle; see equation (4). The beam irradiance, normal to the solar beam, G_{b0} (W/m^2) is attenuated by the cloudless atmosphere, and calculated as follows:

$$G_{b0c} = G_0 \exp\{-0.8662T_{LK}m\delta_R(m)\} \quad (8)$$

The term $0.8662T_{LK}$ is the Linke atmospheric turbidity factor [dimensionless] corrected by [20]. Subindex c shows that we are calculating clear sky irradiances. The parameter m in (8) is the relative optical air mass calculated using the formula [21],

$$m = \frac{p/p_0}{\sin h_0^{ref} + 0.50572(h_0^{ref} + 6.07995)^{-1.6364}} \quad (9)$$

where h_0^{ref} is the solar altitude in degrees corrected by the atmospheric refraction component Δh_0^{ref} , and p/p_0 is a correction for a given elevation z .

Taking into account what written above, the beam irradiance on a horizontal surface $G_b(0)$ becomes,

$$G_{bc}(0) = G_{b0c} L_f \sin h_0 \quad (10)$$

where h_0 is the solar altitude angle and L_f , the lighting factor that corrects the beam irradiance as the surface is sunlit or shadowed. Then the beam irradiance on an inclined surface $G_b(\beta)$ is obtained as,

$$G_{bc}(\beta) = G_{b0c} L_f \sin \delta_{exp} \quad (11)$$

where β is the angle between the inclined surface and the horizontal, and δ_{exp} is the solar incidence angle measured between the sun beam direction and its projection on an inclined surface. Note that, for horizontal surfaces, δ_{exp} coincides with h_0 .

3.1.2 Diffuse radiation

The estimation of the diffuse component in sunlit or shadowed horizontal surfaces $G_{dc}(0)$ (W/m^2) is carried out using the equation,

$$G_{dc}(0) = G_0 T_n(T_{LK}) F_d(h_0) \quad (12)$$

where $G_{dc}(0)$ is a function of the diffuse transmission T_n which only depends on the Linke turbidity factor T_{LK} and on a function F_d depending on the solar altitude h_0 [22].

The transmission function $T_n(T_{LK})$ will be,

$$T_n(T_{LK}) = -0.015843 + 0.030543T_{LK} + 0.0003797T_{LK}^2 \quad (13)$$

And, $F_d(h_0)$,

$$F_d(h_0) = A_1 + A_2 \sin h_0 + A_3 \sin^2 h_0 \quad (14)$$

where the values of A_1 , A_2 and A_3 depend only on the turbidity T_{LK} . On the other hand, the procedure for obtaining the clear-sky diffuse irradiance on a inclined surface with an inclination angle γ_N , $G_d(\gamma_N)(W/m^2)$ considers both sunlit and shadowed surfaces (see section 2) following the equations proposed in [23]. For sunlit surfaces ($L_f = 1$) the equations are,

If $h_0 \geq 0.1$ radians

$$G_{dc}(\gamma_N) = G_{dc}(0) \left(F(\gamma_N)(1 - K_b) + K_b \frac{\sin \delta_{exp}}{\sin h_0} \right) \quad (15)$$

If $h_0 < 0.1$ radians

$$G_{dc}(\gamma_N) = G_{dc}(0) [F(\gamma_N)(1 - K_b) + (K_b \sin \gamma_N \cos A_{LN}) / (0.1 - 0.008h_0)] \quad (16)$$

where $A_{LN}^* = A_0 - A_N$

if $-\pi \leq A_{LN}^* \leq \pi$ then $A_{LN} = A_{LN}^*$

if $A_{LN}^* > \pi$ then $A_{LN} = A_{LN}^* - 2\pi$

if $A_{LN}^* < -\pi$ then $A_{LN} = A_{LN}^* + 2\pi$

For shadowed surfaces ($L_f < 1$).

$$G_{dc}(\gamma_N) = G_{dc}(0)F(\gamma_N) \quad (17)$$

where $F(\gamma_N)$ is a function defined for the diffuse sky irradiance that may be computed as,

$$F(\gamma_N) = r_i(\gamma_N) + N \left(\sin \gamma_N - \gamma_N \cos \gamma_N - \pi \sin^2 \frac{\gamma_N}{2} \right) \quad (18)$$

being $r_i(\gamma_N)$ a fraction of the sky dome viewed by an inclined surface,

$$r_i(\gamma_N) = (1 + \cos \gamma_N) / 2 \quad (19)$$

The value of N for shadowed surfaces is 0.25227 while, for sunlit surfaces under clear sky, it is defined as,

$$N = 0.00263 - 0.712K_b - 0.6883K_b^2 \quad (20)$$

K_b is a proportion between beam irradiance and extraterrestrial solar irradiance on a horizontal surface,

$$K_b = G_{bc}(0)/G_0(0) \quad (21)$$

where

$$G_0(0) = G_0 \sin h_0 \quad (22)$$

3.1.3 Reflected radiation

The last component to take into account is the ground reflected irradiance under clear sky ($G_r(\gamma_N)$). According to [24], this will be proportional to the global horizontal irradiance $G_c(0)$, to the mean ground albedo ρ_g and a fraction of the ground viewed by an inclined surface $r_g(\gamma_N)$.

$$G_r(\gamma_N) = \rho_g G_c(0) r_g(\gamma_N) \quad (23)$$

where

$$r_g(\gamma_N) = (1 - \cos \gamma_N)/2 \quad (24)$$

$$G_c(0) = G_{bc}(0) + G_{dc}(0) \quad (25)$$

3.2 Solar radiation under real-sky

Once we have the clear sky radiation values, a correction to obtain the real sky values is necessary. This correction is needed due to the presence of clouds. The values of global radiation on a horizontal surface for real sky conditions $G(0)$ are calculated as a correction of those of clear sky $G_c(0)$ with the clear sky index k_c which has been studied for the island of Gran Canaria [25],

$$G(0) = G_c(0) k_c \quad (26)$$

As some measures of global radiation $G_s(0)$ (where subindex s means *station*) are available at different measurement stations (see 3.3), the value of the clear sky index at each of those points may be computed as,

$$k_c = G_s(0)/G_c(0) \quad (27)$$

At this point we have k_c values only for the measurement stations. The next step will be the interpolation of the index for the whole zone. A simple formula that has also been used in other environmental problems defined on complex orography (see, e.g., [26]) is applied,

$$k_c = \varepsilon \frac{\sum_{n=1}^N \frac{k_{cn}}{d_n^2}}{\sum_{n=1}^N \frac{1}{d_n^2}} + (1 - \varepsilon) \frac{\sum_{n=1}^N \frac{k_{cn}}{|\Delta h_n|}}{\sum_{n=1}^N \frac{1}{|\Delta h_n|}} \quad (28)$$

where k_c corresponds to the clear sky index at each point of the mesh, k_{cn} is the clear sky index obtained at the measurement stations, N is the number of stations used in the interpolation, d_n is the horizontal distance and $|\Delta h_n|$ is the difference in height between station n and the studied point, respectively, and ε is a parameter between 0 and 1. In problems with regular orography or in two-dimensional analyses, we choose high values of ε . However, for complex terrains, lower values of ε are a better choice. Thus, since in practice the studied regions often present both regular and irregular zones, an intermediate value of ε is more suitable. We have to include the case where the studied point coincides with a measurement station. In such cases, equation (28) is not continuous. The continuity is ensured if we assume the measured value at those points. To calculate the value of $G_b(0)$ and $G_d(0)$ under real sky, a similar procedure may be applied from experimental measures.

3.3 Typical meteorological year

To obtain the radiation values in real sky conditions we use the measured values in several measurement stations (see 3.2). However, using the values of a single year would take us to a non reliable result since the used data are fruit of the weather conditions in that particular year. To avoid this problem we need an accurate typical meteorological year (TMY). A revision of different methods to obtain it can be seen in [27].

3.3.1 Time series analysis

As we can see in the literature, autoregressive moving average (ARMA) models are widely applied to time series [28]. A series can be adjusted by means of an additive way,

$$Y_t = \sum_i [\alpha_i \cos(\omega i t) + \beta_i \sin(\omega i t)] + \epsilon_t \quad (29)$$

where ω is a constant and the deterministic part of the Y_t variability is a trigonometric series, and the random component, ϵ fits an ARMA model,

$$\epsilon_t = \phi_1 \epsilon_{t-1} + \dots + \phi_p \epsilon_{t-p} + a_t + \theta_1 a_{t-1} + \dots + \theta_q a_{t-q} \quad (30)$$

The model orders are p and q , and its variability depends upon their immediately previous values and a random series, a_t which satisfies the following:

$$E(a_t) = 0 \quad V(a_t) = \sigma_a^2 \quad Cov(a_t, a_{t-k}) = 0 \quad \forall t, k$$

To soften irregularities, moving averages have been used. These ones have been adjusted by the least-squared method. Due to the cyclical character of our series, a Fourier analysis has been chosen. So, Equation (29) becomes:

$$Y_t = \alpha_0 + \sum_{i=1}^r \left[\alpha_i \cos\left(\frac{2\pi i t}{T}\right) + \beta_i \sin\left(\frac{2\pi i t}{T}\right) \right] + \epsilon_t \quad t = 1 \dots n \quad (31)$$

being T the cycle period. Using the moving average method allows to minimize the time series noise transforming Y_t series in another one by means of the following transformation,

$$MY_t = \sum_{j=-m}^m \omega_j Y_{t+j} \quad (32)$$

$$\omega_j = \frac{1}{2m+1} \quad j = -m, \dots, +m$$

being $\omega_{-m} + \dots + \omega_0 + \dots + \omega_m$ the weights for the adjusted series mean. In this example we have chosen a simple weighting function.

To soften the available time series, the Henderson moving average, here M_{21} , has been used. Its amplitude is $2m+1 = 21$, and the weight values are,

$$\omega_j = \frac{\nu_j}{3059} \quad j = -10, -9, \dots, 10$$

3.3.2 Maximum, mean and median trends

TMY describes both, daily global solar irradiation and daily sunshine duration (see [15, 25]). At a considered location, the relevant climatic parameters evolution along the lifetime of the installation can be represented generating characteristic year series by the one year duration temporal series provided by the TMY. We compute the daily typical meteorological year of maximums, means, medians, variance and percentiles of 90% and 75% series of values. In order to improve the knowledge of solar intensities, it was obtained one TMY for each of those series using weight means to smooth the irregular data. Finally, the TMY series were fitted to third grade Fourier series, obtaining excellent results in all the locations around the island.

Once all the TMY series were analyzed, the real trend of the global irradiation behaviour in every location is represented by the median TMY series because means are more susceptible to spurious data. Most of the days present a clear sky condition in the island southern stations, so median TMY series are quite regular and similar, following an annual tendency without many disturbing values. In Las Palmas de Gran Canaria and Gáldar (northern stations), the irradiation suffers a descent during the summer months. This effect is caused by the cloudiness generated by the Trade Winds along the northern face of the island. Although Sta. Brígida is on the northern face of the island, the cloudiness in the summer months doesn't affect it because of its higher altitude.

The proposed model to represent daily time series for radiation is:

$$\frac{T_d - Z_{ad}}{s_d} - M = z_{ad} \quad (33)$$

where $d = 1, \dots, 365$ and $a = 1, \dots, A$ being A the number of years with data. M is the average of all the original values Z_{ad} , s_d the series variance, and z_{ad} is the residual ARMA series computed using (30).

For means, we have used the moving average M_{21} ,

$$\hat{m}_d = \frac{1}{A} \sum_{a=1}^A M_{21} Z_{ad} \quad d = 1, 2, \dots, 365 \quad (34)$$

In the other hand, the median series is,

$$M'_d = \text{median}(Z_{ad}) \quad a = 1, \dots, A \quad d = 1, 2, \dots, 365 \quad (35)$$

As always, the Henderson moving average was used,

$$M_d = M_{21} M'_d \quad d = 1, 2, \dots, 365 \quad (36)$$

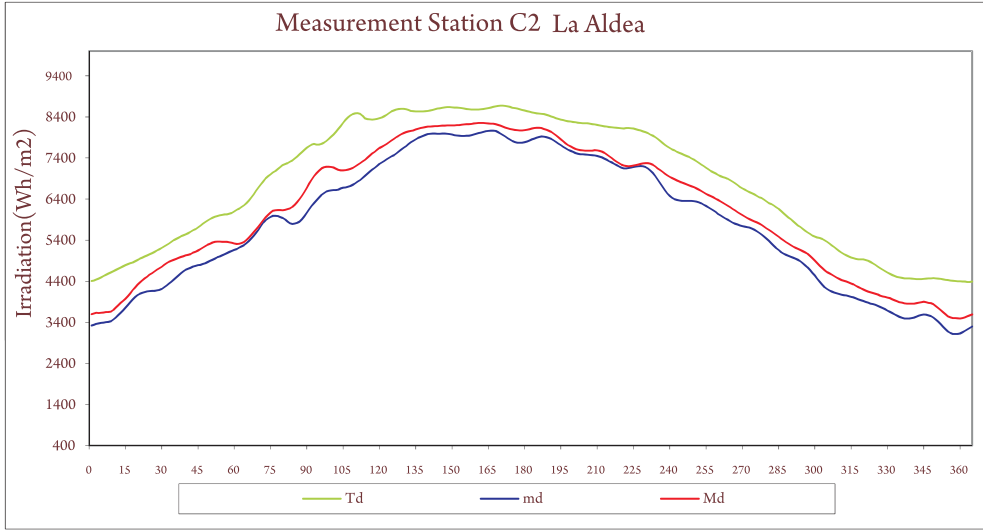


Figure 2: TMY trends

We can see the TMY trends for one of the available measurement stations in Figure 2.

4 Results

Complete radiation results have been obtained for Gran Canaria Island, part of the Canary Islands archipelago. Its coordinates are 28.06° latitude and -15.25° longitude. The UTM coordinates (metres) that define the corners of the considered rectangular domain including the island are (417025, 3061825) and (466475, 3117475), respectively.

Using the refinemet/derefinement parameters as in [4], a mesh with 5866 nodes and 11683 triangles was built to describe the orography and albedo of the island. To define the albedo, the different types of land use in Gran Canaria Island have been studied.

In this simulation, the albedo of the zone varies from 0.05 (Macaronesic laurisilva) to 0.6 (Salt mine). Diffuse radiation calculation implies the need of knowing the Linke turbidity factor. It can be obtained online from the SoDa Service [29] for each month. Beam, diffuse and reflected radiations are computed using the equations presented in section 3, and taking into account the calculated shadow distribution on the mesh. Then, for each day, the clear sky global radiation is computed with the desired time step, as the sum of the three components. In the studied cases, we have chosen a 30 minutes step. We have used Simpson formula to integrate these data numerically in order to obtain the daily radiations.

Once this is done, real sky values are computed using actual radiation data. Seven measurement stations are available with complete data from years 1998 to 2008, for Gran Canaria Island. Table 1 includes their locations. Radiation data have been provided by the Canary Islands Technological Institute (ITC). Since we have computed the typical meteorological year for all the stations [15, 25], real sky radiation values for Gran Canaria Island were obtained for every month.

Table 1: Geolocation of different stations on Gran Canaria Island. Beside latitude, longitude and height (m) of each station place, the corresponding description of village is provided.

Island	label	latitude	longitude	height
Pozo Izquierdo	C0	27.8175 N	15.4244 W	47
Las Palmas de G. C.	C1	28.1108 N	15.4169 W	17
La Aldea de San Nicolás	C2	27.9901 N	15.7907 W	197
San Fernando de M.	C4	27.7716 N	15.5841 W	265
Santa Brígida	C5	28.0337 N	15.4991 W	525
Mogán (village)	C6	27.8839 N	15.7216 W	300
Sardina de Gáldar	C7	28.1681 N	15.6865 W	40

If we take a look at the obtained results, we can see that, under clear sky conditions, beam, diffuse and reflected radiation values are about 82 – 87%, 13 – 18% and 0 – 0.5% of the mean global radiation respectively. The monthly daily average real sky global radiation, for the whole studied region (Gran Canaria Island), varies from 10.6 MJ/m^2 per day in December, to 25.6 MJ/m^2 per day in June (see Figure 3). In this Figure we can see the annual evolution of the computed monthly average per day for both, clear sky and real sky global radiation.

Taking a look at the differences between both curves we obtain Figure 4, where the percentage decrease from the computed radiation is presented. In this Figure we observe the radiation behaviour for Gran Canaria Island, where the most clear days over the whole island are those from Spring, especially during the months of May and June. We can see the typical behaviour of the cloudiness produced by the Trade Winds over the island during Summer. The months of July and August show a separation from the trend that would be expected when we are talking about this season. That

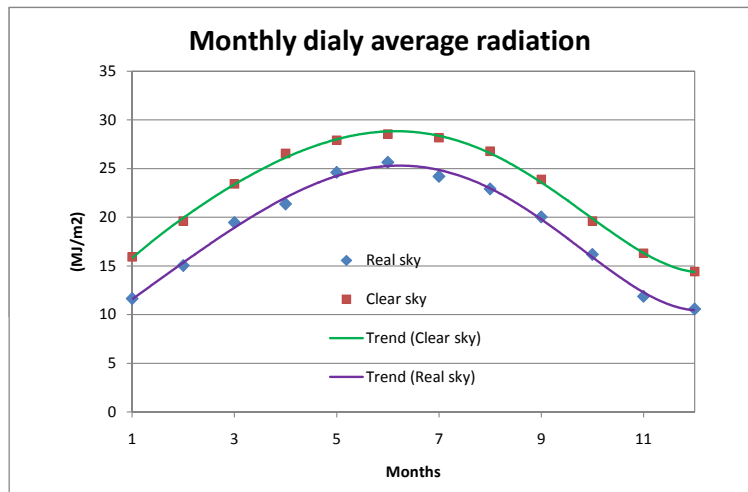


Figure 3: Monthly average radiation per day

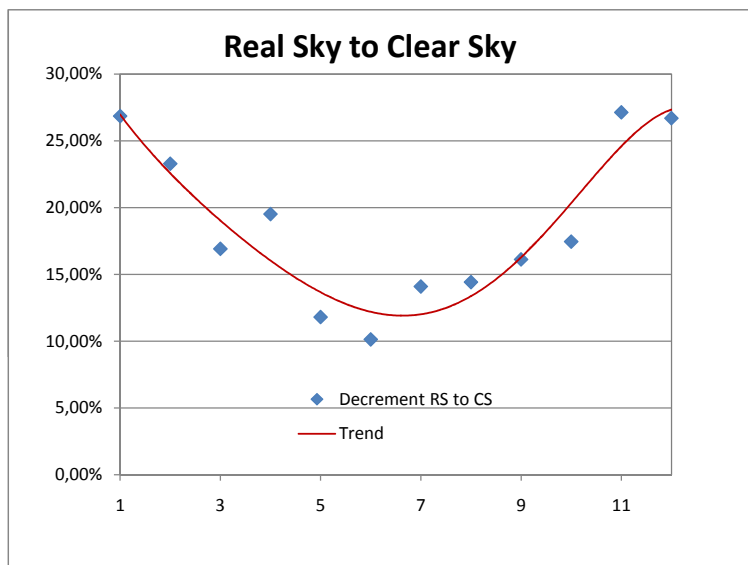


Figure 4: Percentage decrease in computed radiation

decrease in the radiation level over the whole island is caused by the above mentioned cloudiness which affects in Summer to the northern part of the isle.

One month from each season is presented. Figures 5, 6, 7 and 8 show the real sky radiation maps for January, April, July and October. In Figure 7 the effect of the trade winds in the northeastern part of the island can be observed. In this region, a flat zone, the computed radiation is lower than expected due to the cloudiness caused by these winds.

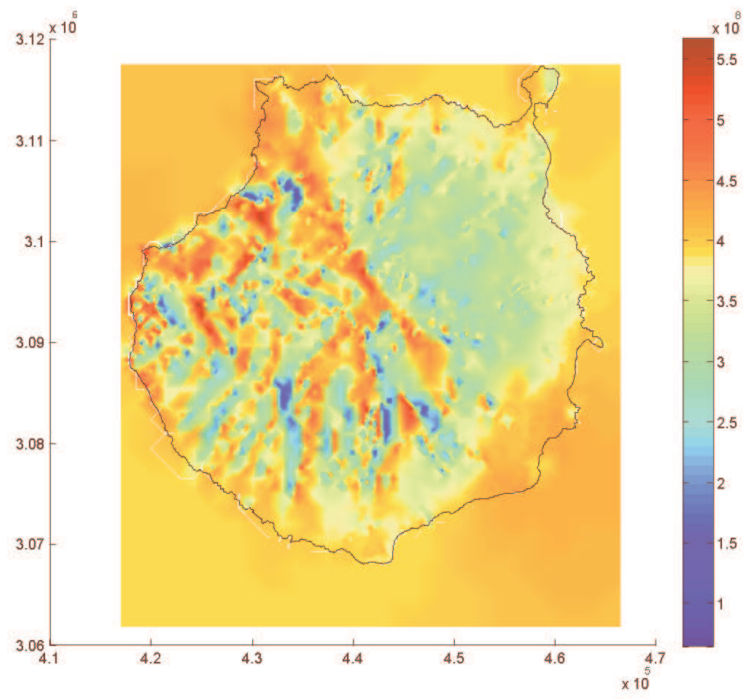


Figure 5: Real sky radiation map for January

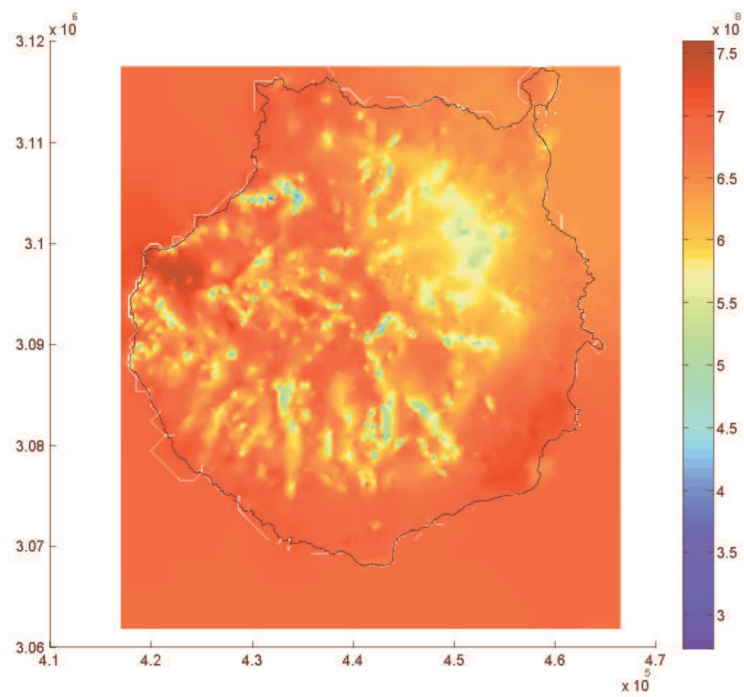


Figure 6: Real sky radiation map for April

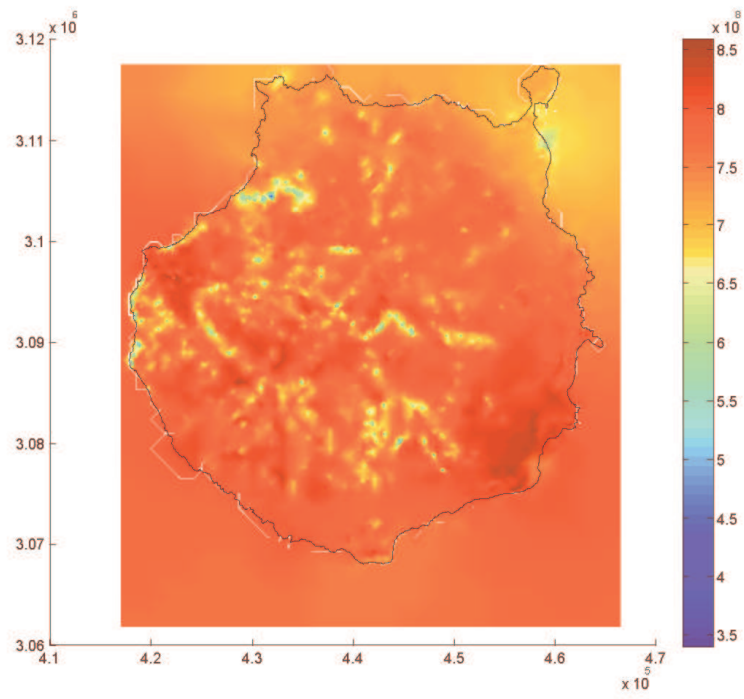


Figure 7: Real sky radiation map for July

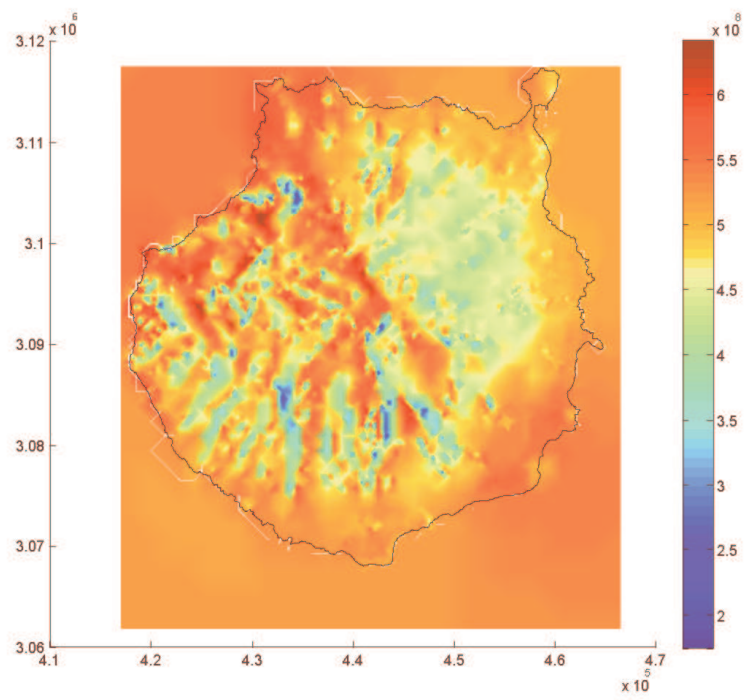


Figure 8: Real sky radiation map for October

5 Conclusions

An improved numerical model for estimating the solar radiation on a surface is proposed. The requirements for a simulation are the location, topography, albedo and observational data. Solar radiation on a surface is estimated taking into account the shadow distribution in each time step. For this purpose, the adaptivity of the triangulation related to the topography and albedo is essential. Adaptive meshes lead to a minimum computational cost, since the number of triangles to be used is optimum [4].

In order to obtain accurate model results, realistic data are needed. The more measurements stations available, the more accurate the results will be. Moreover, statistical treatment of data is necessary to reach accurate conclusions about the possible behaviour of the radiation distribution values for a given place and month. So, a typical meteorological year (TMY) has been computed [15, 25] to serve as departure point to estimate the real sky radiation values. To calculate these, we propose an interpolation method which is suitable when a considerable number of stations is available and they are well distributed in the zone under study. Another procedures, such as spline functions for interpolating the clear sky index on the surface (see e.g. [30]) can be applied.

The developed numerical model allows to choose the most suitable zone in the island, where a solar power station can be placed according to the real sky radiation values. Solar thermal or photovoltaic power generation possibilities are easily estimated starting from the results obtained using the model. As seen in Figures 5 and following, real sky radiation values are available for each and every month from a TMY. This means that solar power generation, photovoltaic or solar thermal, can be estimated from those, taking into account the models of the different power station parts. Moreover, rectangular collectors can be included in the model as composed by two triangles in the same plane. The steps to be followed with these triangles are the same developed for the rest of triangles of the mesh. Therefore, the problem would be reduced to the analysis of the solar radiation on such triangles for a given inclination angle of the southwards-oriented collectors.

The present analysis is done focusing on energy. To make a power analysis, once a single point in the region is chosen, a new computation of the model is needed, stopping in the step prior to the irradiance numerical integration. At this point we have the hourly clear sky distribution of radiation for any day in a month. The irradiation (energy) for each day, in real sky conditions, is now distributed along the sunshine hours of the day, following the clear sky hourly distribution.

References

- [1] M. Šúri, J. Hofierka, “A New GIS-based Solar Radiation Model and its application to photovoltaic assessments”, *Transactions in GIS* 8 (2), 175170. 2004.
- [2] M. Šúri, J. Hofierka, “The solar radiation model for Open source GIS: implementation and applications”. In: Benciolini, B., Ciolli, M., Zatelli, P. (Eds.),

- Proceedings of the Open source GIS-GRASS users conference, Trento, Italy, pp. 1–19, 2002.
- [3] E. Cogliani, P. Ricchiazzi, “Generation of operational maps of global solar irradiation on horizontal plan and of direct normal irradiation from Meteosat imagery by using SOLARMET”, *Solar Energy* 82 (6), 556–562, 2008.
 - [4] G. Montero, J.M. Escobar, E. Rodríguez, R. Montenegro, “Solar radiation and shadow modelling with adaptive triangular meshes”, *Solar Energy* 83 (7), 998–1012, 2009.
 - [5] A. Niewianda, F.D. Heidt, “SOMBRERO: a PC-tool to calculate shadows on arbitrarily oriented surfaces”, *Solar Energy* 58 (4-6), 253–263, 1996.
 - [6] K. Zakšek, T. Podobnikar, K. Oštir, “Solar radiation modelling”, *Computers & Geosciences* 31 (2), 233-170, 2005.
 - [7] J. Dozier, J. Bruno, P. Downey, “A faster solution to the horizon problem”, *Computers & Geosciences* 7, 145–151, 1981.
 - [8] A.J. Stewart, “Fast horizon computation at all points of a terrain with visibility and shading applications”, *IEEE Transactions on Visualization and Computer Graphics* 4 (1), 82–93, 1998.
 - [9] G. Winter, G. Montero, L. Ferragut, R. Montenegro, “Adaptive strategies using standard and mixed finite element for wind field adjustment”, *Solar Energy* 54 (1), 46–56, 1995.
 - [10] L. Ferragut, R. Montenegro, A. Plaza, “Efficient refinement/derefinement algorithm of nested meshes to solve evolution problems”, *Comm Num Meth Engrg* 10, 403–412, 1994.
 - [11] G. Montero, E. Rodríguez, R. Montenegro, J.M. Escobar, J.M. González-Yuste, “Genetic algorithms for an improved parameter estimation with local refinement of tetrahedral meshes in a wind model”, *Advances in Engineering Software* 36, 3–10, 2005.
 - [12] G. Montero, R. Montenegro, J.M. Escobar, E. Rodríguez, J.M. González-Yuste, “Velocity field modelling for pollutant plume using 3-D adaptive finite element method”, *Lecture Notes in Computer Science* 3037, 642–645, 2004.
 - [13] M.C. Rivara, “A Grid Generator Based on 4-Triangles Conforming. Mesh-Refinement Algorithms”, *Int J Num Meth Engrg* 24, 1343–1354, 1987.
 - [14] A. Plaza, R. Montenegro, L. Ferragut, “An improved derefinement algorithm of nested meshes”, *Advances in Engineering Software* 27 (1-2), 51–57, 1996.
 - [15] L. Mazorra, F. Díaz, P. Navarro, “Estimation of global solar radiation by means of sunshine duration”, *Proceedings of ISES Solar World Congress: Solar energy and human settlement, Beijing, China, Vols. I-V*, pp. 2627–2631, 2007.
 - [16] J.W. Gruter (ed), “Radiation Nomenclature”. Brussels, CEC, Second Solar Energy Programme, Project F, Solar Radiation Data, 1984.
 - [17] J. Krcho, “Morfometrická analýza a digitálne modely georeliéfu”, Veda, Bratislava, 1990.
 - [18] M. Jenčo, “Distribúcia priameho slnečného žiarenia na georeliéfe a jej modelovanie pomocou komplexného digitálneho modelu georeliéfu”, *Geografický časopis* 44 (4), 342–354, 1992.

- [19] J.K. Page (ed), “Prediction of Solar Radiation on Inclined Surfaces”, D. Reidel Publishing Co., Dordrecht, 1986.
- [20] F. Kasten, “The Linke turbidity factor based on improved values of the integral Rayleigh optical thickness”, *Solar Energy* 56 (3), 239–244, 1996
- [21] F. Kasten, A.T. Young, “Revised optical air mass tables and approximation formula”, *Applied Optics* 28, 4735–4738, 1989.
- [22] K. Scharmer, J. Greif, “The European Solar Radiation Atlas. Vol. 2 : Database and exploitation software”, Les Presses de l'cole des Mines, Paris, 2000.
- [23] T. Muneer, “Solar Radiation model for Europe”, *Building Services Engineering Research and Technology* 11, 153–163, 1990.
- [24] T. Muneer, “Solar Radiation and Daylight Models for Energy Efficient Design of Buildings”, Architectural Press, Oxford, 1997.
- [25] L. Mazorra, F. Díaz, P. Navarro, F. Déniz, “Accumulated frequency estimation for daily clearness index”, *Proceedings of ISES Solar World Congress: Solar energy and human settlement, Beijing, China, Vols. I-V*, pp. 2632–2635, 2007.
- [26] G. Montero, R. Montenegro, J.M. Escobar, “A 3-D Diagnostic Model for Wind Field Adjustment”, *J Wind Engrg Ind Aer* 74-76, 24917261, 1998.
- [27] A. Argiriou, S. Lykoudis, S. Kontoyiannidis, C. A. Balaras, D. Asimakopoulos, M. Petrakis, P. Kassomenos, “Comparison of methodologies for tmy generation using 20 years data for Athens, Greece”, *Solar Energy* 66 (1), 33–45, 1999.
- [28] R. Aguiar, M. Collares-Pereira, “TAG: A time-dependent, autoregressive, Gaussian model for generating synthetic hourly radiation”, *Solar Energy* 49 (3), 167–174, 1992.
- [29] SoDa Service (Solar Data), “Services for Professionals in Solar Energy and Radiation”. Available at [http : //www.soda – is.com/eng/services/service_invoke/gui.php](http://www.soda-is.com/eng/services/service_invoke/gui.php).
- [30] Y. Xia, M. Winterhalter, P. Fabian, P., “Interpolation of Daily Global Solar Radiation with Thin Plate Smoothing Splines”, *Theor Appl Climatol* 66, 109–115, 2000.